Geomechanics and Engineering, *Vol. 29, No. 5 (2022) 497-508*
https://doi.org/10.12989/gae.2022.29.5.497

Tailings fluidization under cyclic triaxial loading – a laboratory study

Tan Manh Do*[1,2], Jan Laue[1a], Hans Mattson[1b] and Qi Jia[1c]

[1]*Department of Civil, Environmental and Natural Resources Engineering, Luleå university of technology, Luleå, Sweden*
[2]*Department of Civil Engineering, University of Mining and Geology, Hanoi, Vietnam*

(Received January 23, 2022, Revised March 15, 2022, Accepted April 26, 2022)

Abstract. Tailings fluidization (i.e., tailings behave as being fluidized) under cyclic loading is one concern during the construction of tailings dams, especially in the shallow tailings layers. The primary goal of this study is to evaluate the responses of tailings under cyclic loadings and the tailings potential for fluidization. A series of cyclic triaxial undrained and drained tests were performed on medium and dense tailings samples under various cyclic stress ratios (CSR). The results indicated that axial strain and excess pore water pressure accumulated over time due to cyclic loading. However, the accumulations were dependent on CSR values, densities, and drainage conditions. The fluidization potential analysis in this study was then evaluated based on the obtained cyclic axial strain and excess pore water pressure. As a result, tailings samples were stable (unfluidized) under small CSR values, and the critical CSR values, where the tailings fluidized, varied depending on the density of tailings samples. Tailings fluidization is triggered as cyclic stress ratios reach critical values. In this study, the critical CSR values were found to be 0.15 and 0.40 for medium and dense samples, respectively.

Keywords: critical cyclic stress ratios; cyclic characteristics; tailings fluidization

1. Introduction

Tailings, which are often transported and deposited into a tailings impoundment behind dams, are the chief waste stream in the mining industry (Bella 2021, Förstner 1999, Sarsby 2013). In general, tailings are stored in the impoundment, whereas water is discharged via a decant tower (i.e., spillway). In order to avoid tailings to be transported out from the impoundment, porous piers are constructed to make a tailings impoundment and the piers have to be gradually raised (Fig. 1(a)). During the construction of the piers, cyclic loading from the dump haulers would lead to an increase in both undrained strain and excess *PWP* in the tailings below. Due to the cyclic loadings, tailings slurry could be pumped upward to the surface of the piers, so called: tailings pumping. It should be noted that pumping can occur in any type of soil if three conditions are satisfied: (1) cyclic loading; (2) fully saturated soil; and (3) soil with a high percentage of fines (Alobaidi and Hoare 1994; Alobaidi and Hoare 1996). This phenomenon could lead to a decrease of drainage capacity and a reduction in the stability of the overlying granular layers (Christopher *et al.* 2006, Kermani *et al.* 2019). Therefore, tailings pumping (i.e., the migration of tailings slurry from fully saturated tailings into the piers) is one concern during the construction of tailings dams. Such tailings mud pumping often occurs with tailings under as well as on the sides of the piers if tailings behave as being fluidized. Fig. 1(b) shows one example of fluidized tailings pumped upward to the surface of the pier in Aitik tailings dam (Knutsson and Laue 2016).

In general, fluidization due to cyclic traffic loading and seismic-induced liquefaction involve a considerable increase in excess *PWP*. However, the fluidization due to cyclic traffic loading often takes place at shallow depths while the seismic-induced liquefaction happens due to the dynamic accelerations (e.g., earthquake motion) *(Duong et al.* 2013, Indraratna *et al*. 2020, Wheeler *et al.* 2017). During the past decades, the seismic-induced liquefaction has been addressed in many studies on soils by Dash and Sitharam (2011), Kheirbek-Saoud and Fleureau (2012), Sonmezer (2019), Sonmezer *et al.* (2020), Wang *et al.* (2012) or on tailings by Tsuchida (1970), Ishihara *et al.* (1980), Moriwaki *et al.* (1982), Vick (1983), Peters and Verdugo (2003), Wijewickreme *et al.* (2005), Verdugo (2009), James *et al.* (2011), Geremew and Yanful (2012), Festugato *et al.* (2013), Geremew and Yanful (2013), Suazo *et al.* (2016), Hu *et al.* (2017), Zardari *et al.* (2017). However, research on the tailings pumping has not yet been closely evaluated. It should be noted that tailings mud pumping occur in the shallow tailings layers where the tailings behave as being fluidized due to the repetitive (cyclic) loading applied over a considerable period of time as a result of dump haulers driving on the piers of tailings dams. Therefore, one-way cyclic loading (i.e., only cyclic deviatoric compressive stress without reversal stress) is adopted to study the dynamic behavior of tailings.

The present study focuses on the cyclic characteristics

*Corresponding author, Lecturer
E-mail: domanhtan@khoaxaydung.edu.vn
[a]Professor
E-mail: jan.laue@ltu.se
[b]Associate Professor
E-mail: hans.mattsson@ltu.se
[c]Lecturer
E-mail: qi.jia@ltu.se

ISSN: 2005-307X (Print), 2092-6219 (Online)

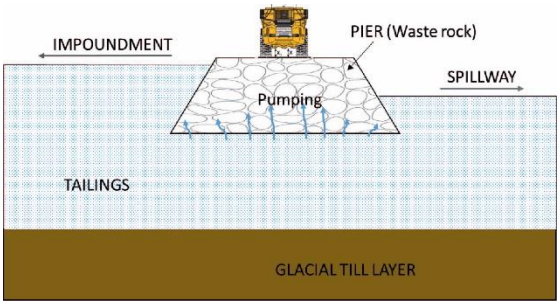

(a)

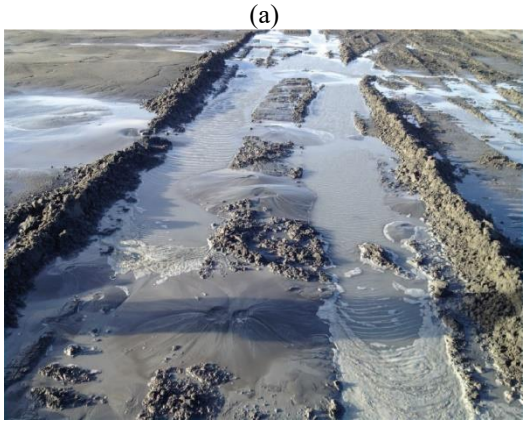

(b)

Fig. 1 Tailings fluidization under cyclic traffic loading: (a) schematic diagram of the process and (b) example of fluidized tailings pumped upward to the surface of the pier (Aitik tailings dam) by Boliden

of tailings utilized for the fluidization potential analysis. A series of cyclic triaxial tests were carried out on medium and dense tailings samples under various cyclic stress ratios (*CSR*). The fluidization potential analysis was then assessed based on the obtained cyclic axial strain and excess *PWP*.

2. Experimental program

Tailings used in the present study originated from a tailings impoundment in Kiruna, Sweden. The tailings are classified as silty sand with 12.7% fine content. Physical properties of the tailings are presented in Table 1. The particle size distribution curves of the tailings studied here and in some other studies are shown in Fig. 2. Tailings samples were prepared by using the under compaction method and targeted to dry densities of 1700 kg/m^3 (medium samples) and 1810 kg/m^3 (dense samples). This method has been successfully employed in many previous studies as it could consider the compaction energy transferring from upper layers to bottom layers (Bedin *et al.* 2012, Indraratna *et al*. 2020, Kwan and Mohtar 2018, Ladd 1978, Lade 2016, Shajarati *et al.* 2012). The tailings at the optimum moisture content was compacted into a manufactured mould (50 × 100 mm) (Fig. 3). Tailings sample preparation the under compaction method is discussed in detail in the study by the authors (Do 2021). In brief, same amount of tailings was compacted into five layers. The height of each layer was experimentally pre-determined by testing the dry density variations with respect

Table 1 Physical properties of tailings used in this study

Properties	Tailings
Maximum dry density (kg/m^3)	2015
Optimum Moisture Content (%)	10.9
Maximum void ratio	1.05
Minimum void ratio	0.49
Specific gravity	3.01
D_{50} (mm)	0.187
Fine content (%)	12.7
Colour	Dark green

to the distance from the bottom of the specimen. In this study, the heights from the bottom to the top of five layers were determined as 20.4 mm, 20.35 mm, 20.15 mm, 19.8 mm, and 19.3 mm. Pre-determined quantities of tailings were spread carefully and sequentially in the five layers into the mould. Each layer was then densified by tamping with a steel rod that was marked for five designated portions.

For all tailings samples used in cyclic triaxial tests, the minimum back pressure of 600 kPa was utilized to assist the specimen in reaching full saturation. The samples were then consolidated to the low effective confining pressure of 30 kPa, representing the condition of the shallow tailings layers. After that, all tailings samples were sheared cyclically by using the one-way stress-controlled loading scheme under various cyclic stress ratios (*CSR*)

$$CSR = \frac{q_{cyc}}{2 \times \sigma_c'} \quad (1)$$

where q_{cyc} is the amplitude of cyclic part of the deviatoric stress and σ_c' is the effective confining pressure.

For each cyclic triaxial test, the targeted cyclic stresses were controlled by setting values (Geosys software) varied from an initial deviatoric stress of 10 kPa (i.e., from anisotropic consolidation) to a value of (10 + q_{cyc}) kPa. The bottom drainage valve was used to control the drainage conditions during shearing phases (i.e., kept closed for the undrained cyclic triaxial loading or kept opened for the drained cyclic triaxial loading).

It should be noted that this stress-controlled loading has been widely used for cyclic characteristics of soils under traffic loading in many previous studies (Baki *et al*. 2012, Cai *et al.* 2013, Gu *et al*. 2016, Indraratna *et al.* 2020, Moses *et al.* 2003). The procedures in ASTM Standards (D 5311) were used to perform the cyclic triaxial tests in this study. The experimental program is presented in detail in Table 2. The tested CSR values varied from 0.12 to 0.40 and 0.25 to 0.70 for medium and dense tailings samples, respectively. The frequency *f*=1 Hz is chosen in this study, based on the fact that the speed of dump haulers driving on the pier is typically limited to 40 km/h (Knutsson and Laue 2016, Wheeler *et al.* 2017). The cyclic triaxial tests were terminated after reaching either 5% cyclic axial strain or 1000 cycles.

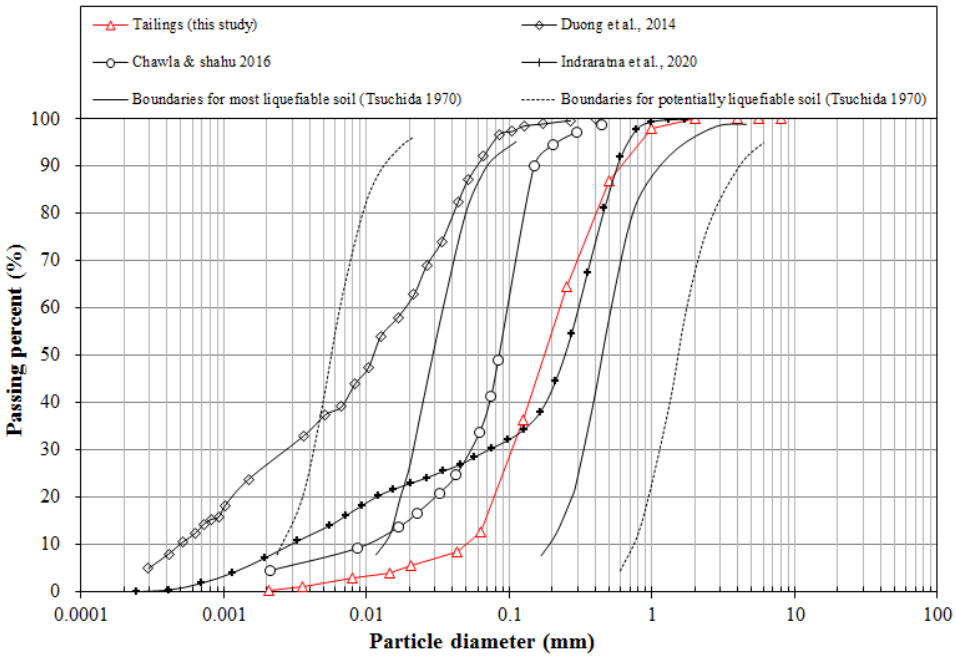

Fig. 2 Particle size distribution curves of tailings used in this study and in other similar studies

Fig. 3 A manufactured mould (50 × 100 mm) for the under compaction method

3. Results and discussion

In order to get a general idea of the cyclic response of tailings materials, a standard four-way plot of tailings sample *CRS*=0.3, Medium is shown in Fig. 4. For better clarity, only first 20 cycles of the test are plotted. The standard four-way plot usually consists of four subfigures: stress path (Fig. 4(a)), stress-strain curves (Fig. 4(b)), development of excess pore pressure ratio (Fig. 4(c)) and (d) development of shear strain (Fig. 4(d)), so-called standard four-way plot (Kammerer *et al*. 2002). As can be seen, the axial strain (Figs. 4(b), 4(d) and excess *PWP* ratio (Fig. 4(c)) accumulated over time due to cyclic loading. Due to the development of excess *PWP* (i.e., involving the development of excess *PWP* ratio), the effective stress of the tailings sample decreased after each single cycle (Fig. 4(a)).

3.1 Cyclic characteristics of tailings

Fig. 5 illustrates the undrained cyclic axial strain response of tailings samples (i.e., both medium and dense). As can be seen, the cyclic axial strains of these samples increased with respect to the number of cycles. However, the cyclic axial strain response was significantly dependent on the *CSR* values, regardless of densities. In particular, at low *CSR* values of 0.12 (medium sample) and 0.25 (dense sample), the cyclic axial strains increased slightly and reached 0.24% (medium sample) and 0.12% (dense sample) after 1000 cycles. However, at higher *CSR* values (i.e., *CSR* ≥ 0.15 for medium and *CSR* ≥ 0.40 for dense samples), the cyclic axial strain increased dramatically up to 5% (fluidized sample) after a certain number of cycles. This trend is consistent with findings from other studies despite different materials used (Baki *et al.* 2012,

Table 2 Experimental program used for cyclic triaxial tests on tailings samples

Initial dry density	Relative density, *Dr*	Confining pressures, σ_c'	Cyclic stress ratio, *CSR*	Frequency (Hz)	Drainage conditions
(kg/m^3)	(%)	(kPa)			
1700	51	30	0.12	1	Undrained and drained cyclic triaxial loading
1700	51	30	0.15	1	Undrained and drained cyclic triaxial loading
1700	51	30	0.25	1	Undrained and drained cyclic triaxial loading
1700	51	30	0.30	1	Undrained and drained cyclic triaxial loading
1700	51	30	0.40	1	Undrained and drained cyclic triaxial loading
1810	70	30	0.25	1	Undrained cyclic triaxial loading
1810	70	30	0.40	1	Undrained cyclic triaxial loading
1810	70	30	0.50	1	Undrained cyclic triaxial loading
1810	70	30	0.60	1	Undrained cyclic triaxial loading
1810	70	30	0.70	1	Undrained cyclic triaxial loading

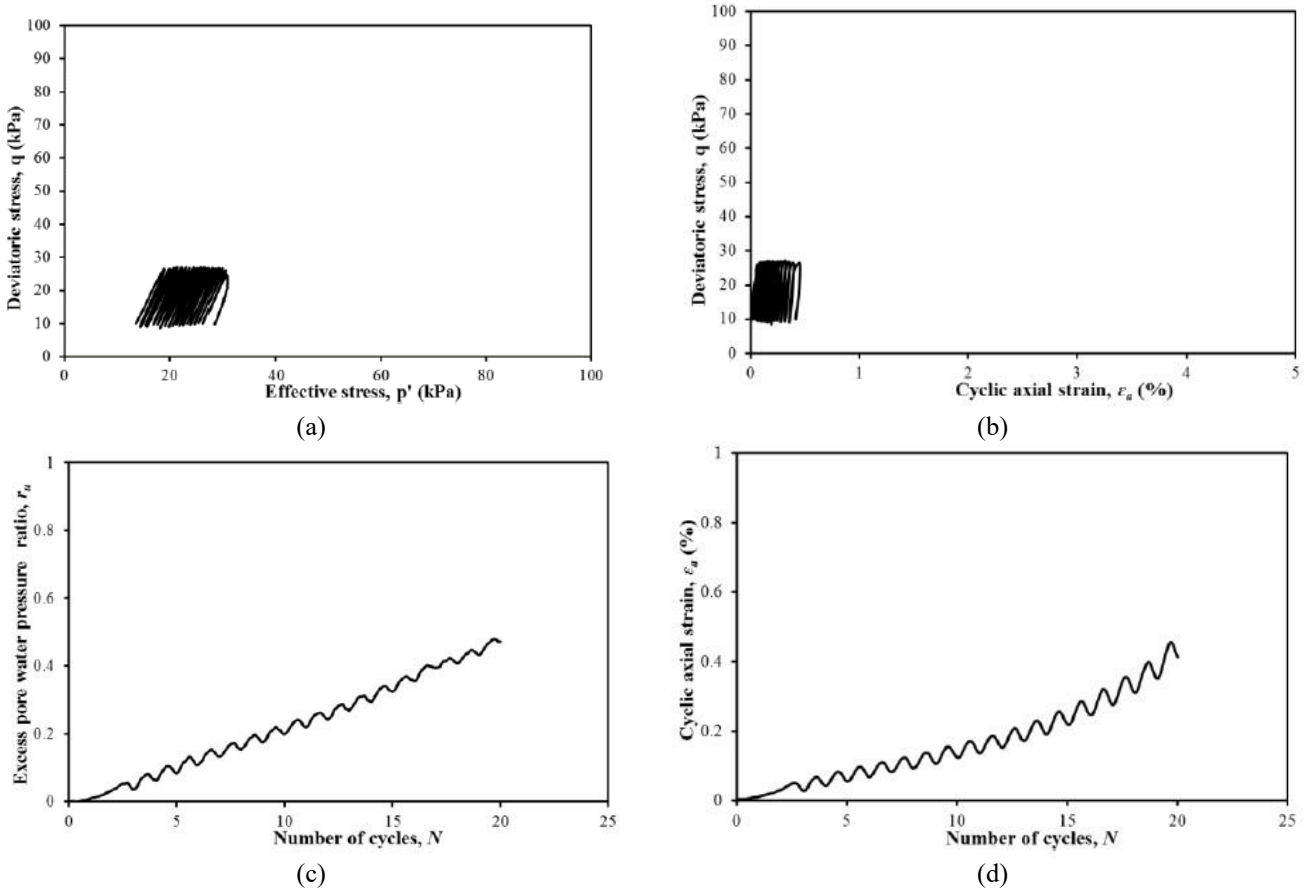

Fig. 4 Standard four-way plot of tailings sample CRS=0.3, Medium: (a) stress path, (b) stress-strain curves, (c) development of excess pore pressure ratio and (d) development of shear strain

Indraratna *et al.* 2020, Selig and Chang 1981, Wang *et al.* 2017). (a) The excess *PWP* response of tailings samples under undrained cyclic loading is presented as residual *PWP* ratios against number of cycles (Fig. 6). The idea of

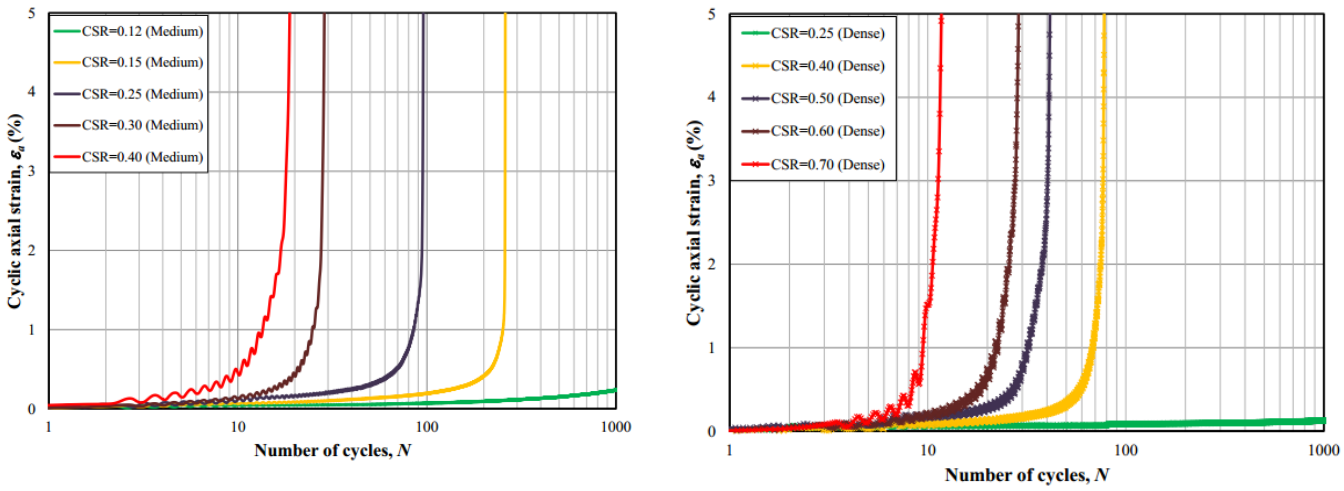

(a) (b)

Fig. 5 Undrained cyclic axial strain response of (a) medium tailings samples and (b) dense tailings samples

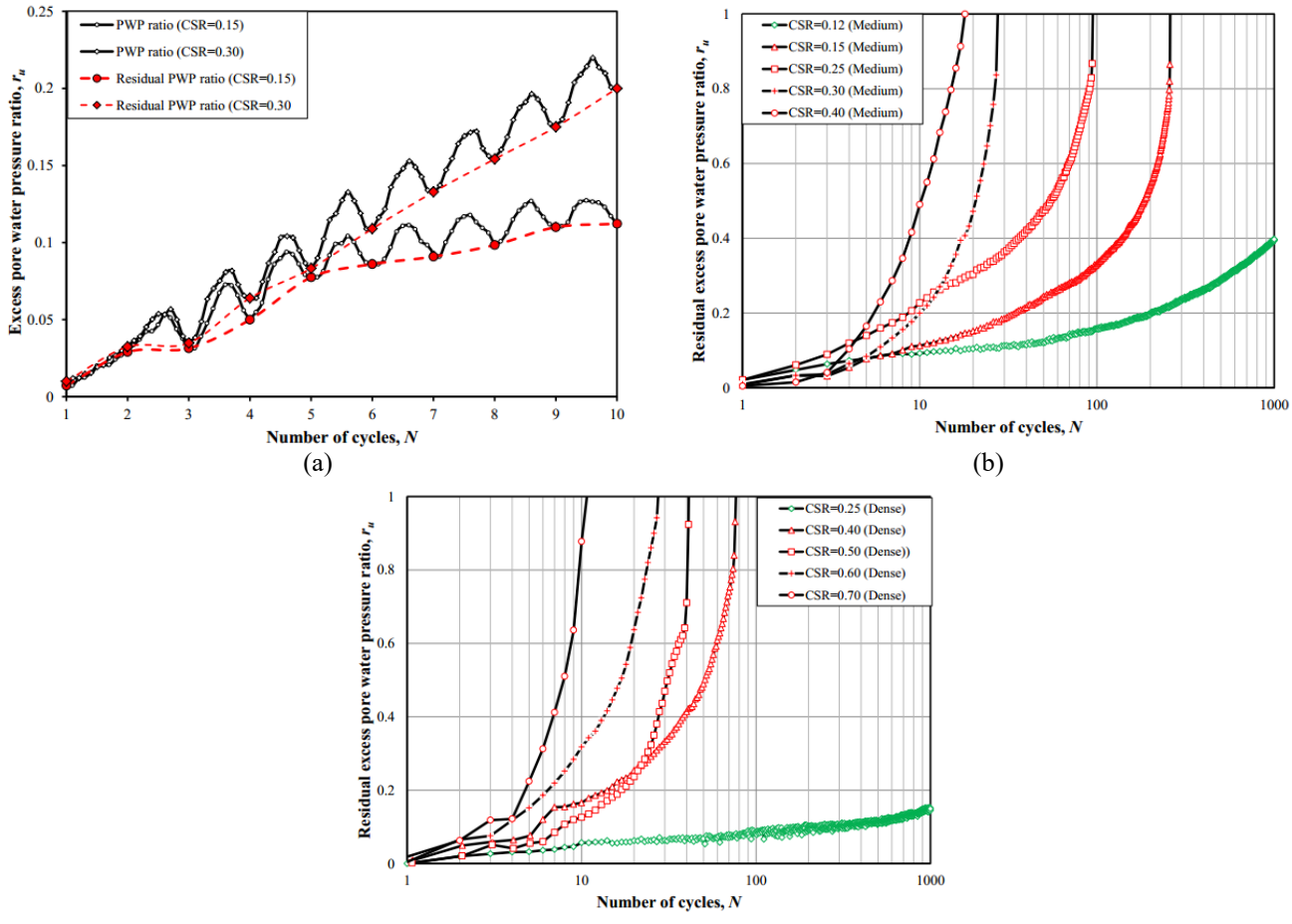

(a) (b)

(c)

Fig. 6 The excess *PWP* response under undrained cyclic loading: (a) idea of the residual excess *PWP* ratio; (b) medium tailings samples and (c) dense tailings samples

the residual *PWP* ratios (i.e., the troughs of each cycle) is presented in Fig. 6(a). The excess *PWP* response is represented by the excess pore water pressure ratios (r_u), which is well known as the ratio between excess pore pressure development and the initial effective stress. As shown in Figs. 6(b) and 6(c), the development of *PWP* followed the same trend as for the axial strain, regardless of densities and *CSR* values. When *CSR* was small (i.e., *CSR* = 0.12 for medium and *CSR* = 0.25 for dense samples), r_u increased and reached 0.39 and 0.15, respectively. However,

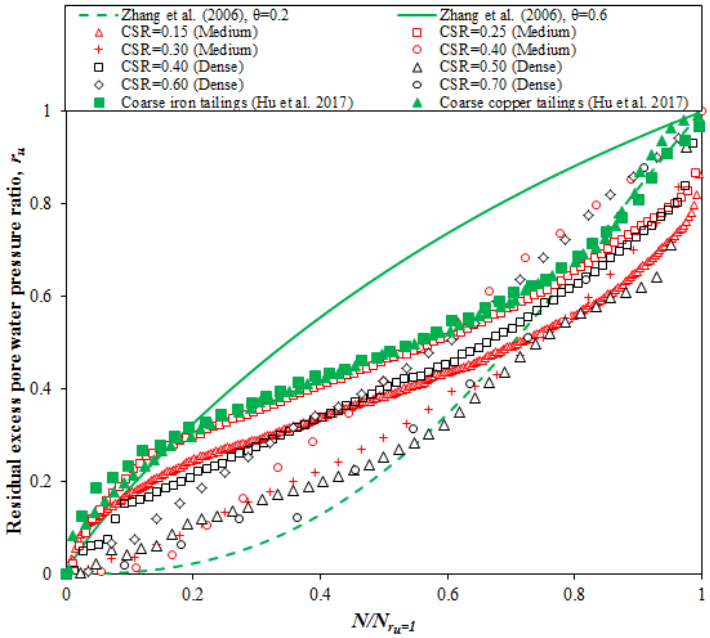

Fig. 7 Relationship between excess PWP ratio (r_u) and the number of cycles (N) normalised by the number of cycles at r_u=1

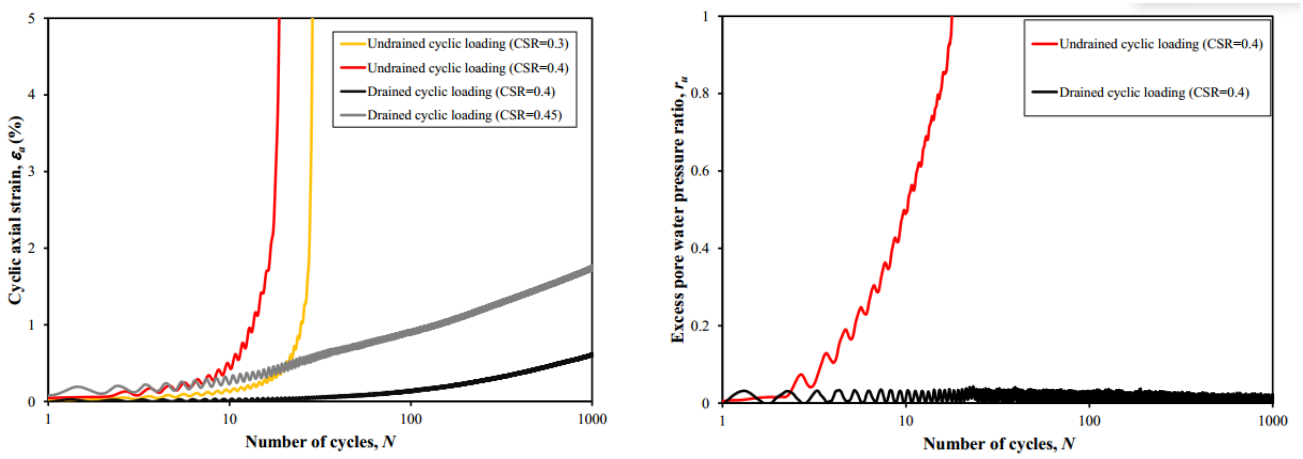

(a) (b)

Fig. 8 Cyclic characteristics of selected medium tailings samples with different drainage conditions: (a) cyclic axial strain vs number of cycles and (b) excess *PWP* ratio vs number of cycles

when *CSR* was higher (i.e., *CSR* ≥ 0.15 for medium and *CSR* ≥ 0.40 for dense samples), r_u grew rapidly up to 1.0 at an early stage. It should be noted that r_u=1.0 means soil liquefaction during cyclic loading. In addition, the samples with higher relative density tended to resist cyclic loads better than those with lower relative density under the same loading conditions. Take CSR = 0.25 as an example, while the excess pore water pressure ratio of CRS=0.25 (Medium) raised rapidly and reached 1.0 after only 95 cycles (failure), that of CRS=0.25 (Dense) increased slightly and reached only 0.15 after 1000 cycles (not failure). Take CSR=0.40 as another example; the excess pore water pressure ratios of both CRS=0.40 (Medium) and CRS=0.40 (Dense) reached 1.0. However, in order to reach ru=1.0, the sample with higher relative density, i.e., CRS=0.40 (Dense) took more number of cycles (77 cycles) than sample with lower relative density, i.e., CRS=0.40 (Medium) (18 cycles).

Fig. 7 illustrates the relationship between r_u and the number of cycles (N) normalised by the number of cycles at r_u=1 ($N_{ru=1}$). For reference, data in this study are compared to those from the literature for various tailings types (Hu *et al.* 2017, Zhang *et al.* 2006). Note that Zhang *et al.* (2006) proposed a model to predict cyclic pore pressure based on various undrained cyclic triaxial tests of tailings materials, which is expressed as

$$r_u = \frac{4}{\pi}\arctan\left(\frac{N}{N_{r_{u=1}}}\right)^{1/2e} \quad (2)$$

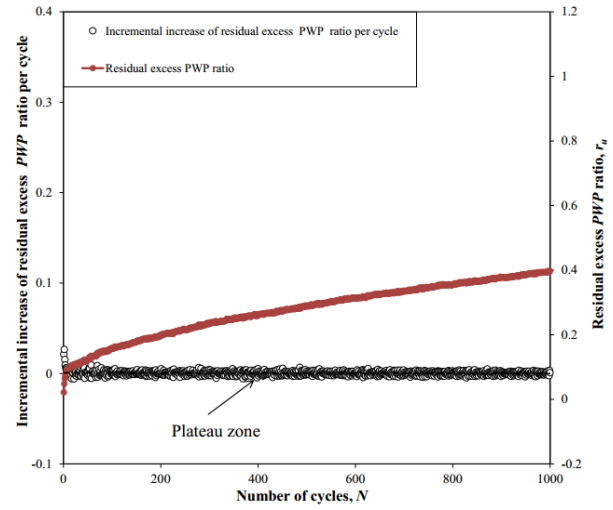

(a)

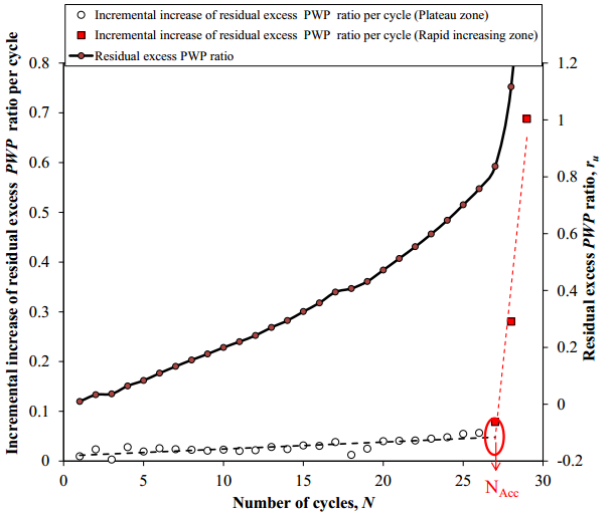

(b)

Fig. 9 Incremental increase of excess *PWP* ratio of the selected tailings samples: (a) unfluidized tailings sample and (b) fluidized tailings sample

where θ is an empirical constant determined from laboratory testing.

As shown, the data in this study fall into the pore water pressure envelope by Zhang *et al.* (2006) with the optimal values of θ=0.2 (lower bound) and θ=0.6 (upper bound). In addition, compared to the dense tailings samples, the data of the medium tailings samples are closer to those reported by Hu *et al.* (2017). The data of dense tailings samples are shifted downwards due to a lower rate of excess pore pressure generated in the earlier cycles, as observed in Fig. 6 (at the same CSR). Note that the densities of coarse tailings used by Hu *et al*. (2017) are relatively low, ranging from 1460 to 1600 kg/m^3.

In addition to *CSR* and density, the cyclic characteristics of tailings are also affected by the drainage conditions. Fig. 8 shows the cyclic characteristics of selected medium tailings samples with different drainage conditions. The results obtained from the tests with *CSR* = 0.3; 0.4 (undrained tests), and *CSR*=0.4; 0.45 (drained tests) are plotted in Fig. 8(a). As can be seen, the development of drained cyclic axial strain was relatively small despite the increasing number of cycles *N* up to 1000 cycles. However, the undrained cyclic axial strain accumulated rapidly up to 5% (fluidized tailings sample) after a limited number of cycles. This is due to the considerable development of excess *PWP* under undrained cyclic loading, the main factor in failure of tailings samples. Take *CSR* = 0.4 as an example (Fig. 8(b)), while r_u of the undrained test raised rapidly and reached 1.0 after only 18 cycles, r_u of the drained test almost remained constant up to 1000 cycles.

3.2 Tailings fluidization under cyclic triaxial loading

The build-up of excess *PWP* under cyclic loading has an important effect on the migration of fluidized subgrade materials (Alobaidi and Hoare 1994, Alobaidi and Hoare 1996, Duong e*t al.* 2013, Indraratna *et al*. 2020, Kermani *et al.* 2019). Additional insight into the development of excess

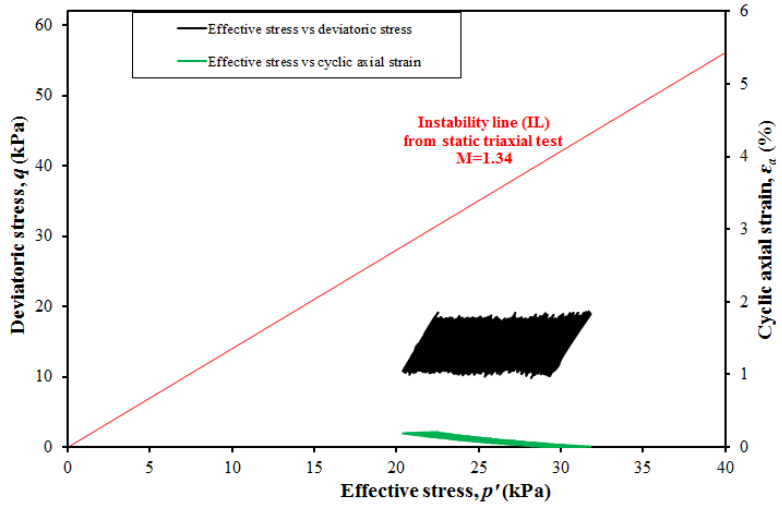

(a)

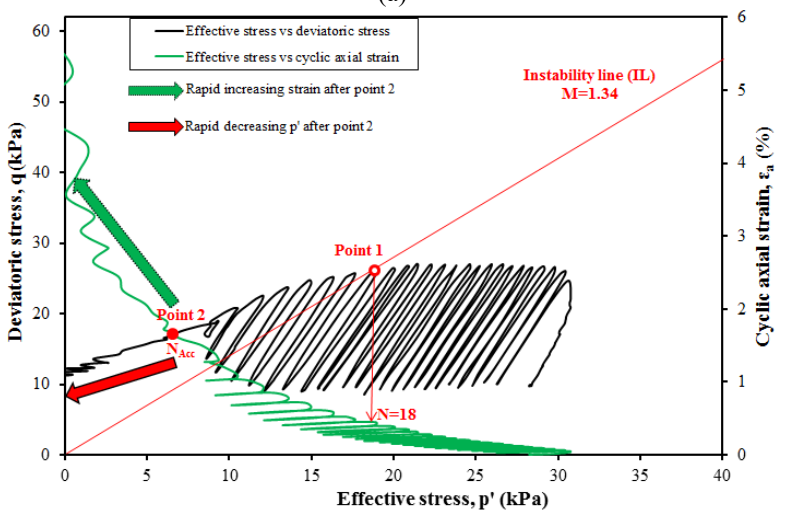

(b)

Fig. 10 Typical stress paths of the selected tailings samples: (a) unfluidized tailings sample and (b) fluidized tailings sample

PWP can be attained by looking into the incremental increase of excess *PWP* ratio per cycle. The incremental increases of excess *PWP* ratio of the selected medium tailings samples are shown in Fig. 9(a) (unfluidized tailings sample; *CSR*=0.12) and Fig. 9(b) (fluidized tailings sample; *CSR*=0.30). For the unfluidized tailings sample, it can be clearly observed a plateau zone characterised by an almost constant incremental increase of excess *PWP* ratio per cycle despite an increase in the number of cycles up to 1000 (Fig. 9(a)). For the fluidized tailings sample, the incremental increase was separated into two zones: (a) plateau zone with an almost constant incremental increase of excess *PWP* ratio; and (b) rapid increasing *PWP* zone in which the incremental increase was accelerated until sample failure. A critical point, N_{Acc}, which is the number of cycles at which the incremental increase starts accelerating, is identified in Fig. 9(b).

In addition to the incremental increase of excess PWP, two typical stress paths are illustrated in the q-p' planes for both selected stable and unstable tests (Fig. 10). In Fig. 10, the instability line (IL) is defined from the results of a static triaxial compression test. As expected, the stress path of the stable test falls well below the IL. A relatively small cyclic axial strain (0.24% after 1000 cycles) (Fig. 10(a)) would be explained for the stability of this test. However, it can be seen from Fig. 10(b), the stress path of the unstable test moves towards and crosses the IL (point 1) by the cyclic axial strain of 0.35% (after 18 cycles). It follows by a loss of stability with decreases in both deviator stress and effective stress. These results are in good agreement with those of the study by Baki *et al.* (2012) and Vernay *et al.* (2016), addressing the cyclic instability of sand under one-way cyclic loading. In Fig. 10(b), the critical point (N_{Acc}), at which the incremental increase starts accelerating as presented in Fig. 9(b), is linked and marked as point 2. The corresponding effective stress and cyclic axial strain at this critical point are 6.68 kPa and 1.63%, respectively. After passing this critical point, a rapid increase in the cyclic axial strain (strain-softening) along with the significant reduction of effective stress (p') can be observed. In this sense, the sample gets fluidized after the critical point (N_{Acc}) and then

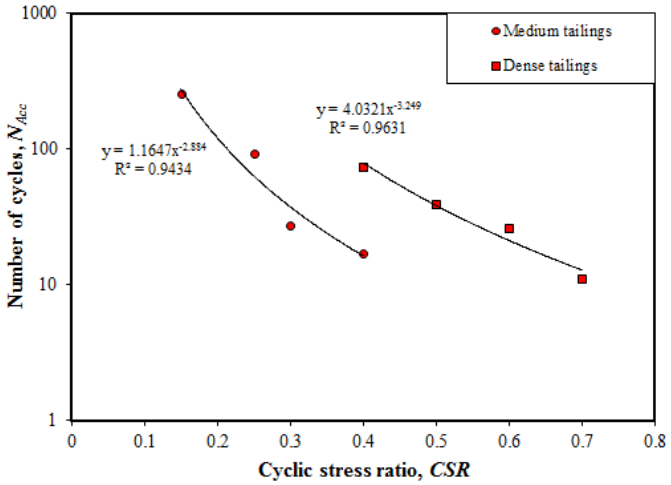

Fig. 11 Relationship between N_{Acc} and *CSR*

collapses. A rapid increase in excess *PWP* and cyclic axial strain under undrained cyclic loading has also been found in the previous study on subgrade fluidization (Indraratna *et al.* 2020). Their study has reported that the fluidization involves the rapid decrease in the deviator stress due to a significant amount of strain-softening. In addition, the same observations on the strain-softening can also be found in the one-way cyclic instability of sand (Baki *et al.* 2012, Li *et al.* 2017, Vernay *et al*. 2016) and silt (Hyde *et al*. 2006).

Eventually, a relationship between N_{Acc} and *CSR* is shown in Fig. 11. As can be observed, an increased N_{Acc} can be achieved with either a decreased *CSR* value or an increased density. A non-linear relationship between *CSR* and N_{Acc} was found in the form of

$$N_{Acc} = a \times CSR^{-b} \quad (3)$$

In this study, the parameters in Eq. (3) were found to be a_1= 1.165; b_1= 2.88 (medium tailings), a_2= 4.032; b_2= 3.25 (dense tailings). With these parameters, *CSR* can be used for the evaluation of N_{Acc}. However, these parameters could be affected by tailings types. Therefore, the relation in Eq. (2) is expected to be validated to other tailings in future work.

4. Conclusions

A laboratory study on cyclic characteristics of tailings for a fluidization potential analysis was conducted. Based on the results of this study, the following conclusions can be drawn:

- Axial strain and excess *PWP* accumulated over time due to cyclic loading. However, the accumulations were significantly dependent on *CSR* values, densities, and drainage conditions.

➢ The cyclic axial strain and excess pore water pressure increase slightly at low CSR values (i.e., CSR = 0.12 for medium and CSR = 0.25 for dense samples) even after 1000 cycles. However, at higher CSR values (i.e., CSR ≥ 0.15 for medium and CSR ≥ 0.40 for dense samples), these values increase dramatically, and samples get failure after a limited number of cycles. This is consistent with the data report in the literature.

➢ The development of strain and excess pore water pressure is relatively insignificant under the drained cyclic loading despite the increasing number of cycles N up to 1000. However, these values under the undrained condition accumulate rapidly, and samples get failures after a limited number of cycle (i.e., with the same CSR). This is due to the considerable development of PWP under undrained cyclic loading, the main factor in the failure of tailings samples.

- The concept of tailings fluidization was studied by looking into the incremental increase of excess *PWP* ratio per cycle. An unfluidized sample was identified with a plateau zone characterised by an almost constant incremental increase of excess *PWP* ratio (i.e., consistent with the insignificant developments of cyclic axial strain and excess *PWP*). For a fluidized sample, the incremental increase was separated into two zones: (a) plateau zone; (b) rapid increasing excess *PWP* zone. This finding links to a rapid increase in the cyclic axial strain (strain-softening) along with the significant reductions of deviator stress and effective stress observed in the corresponding stress paths.
- The critical point (N_{Acc}), the number of cycles at which the incremental increase starts accelerating until the sample is fluidized, was then employed for presenting a relation between the cyclic stress ratio (*CSR*) and the number of cycles N_{Acc}. As a result, an increased N_{Acc} can be achieved with either a decreased *CSR* value or an increased density.

Acknowledgments

This research was funded by the Swedish transport administration (Trafikverket), the Swedish joint research program for road and railway geotechnology Bransch-samverkan i grunden (BIG), Swedish Hydropower Centre (SVC), and Luleå University of Technology. The research

presented in this paper was carried out as a part of the Swedish Hydropower Center (Svenskt Vattenkraftscentrum, SVC). SVC has been established by the Swedish Energy Agency, Energiforsk, and Svenska Kraftnät, together with Luleå University of Technology, KTH Royal Institute of Technology, Chalmers University of Technology, Uppsala University, and Lund University. The participating companies and industry associations are: Andritz Hydro, Boliden, Fortum Sweden, Holmen Energi, Jämtkraft, Karlstads Energi, LKAB, Mälarenergi, Norconsult, Rainpower, Skellefteå Kraft, Sollefteåforsens, Statkraft Sverige, Sweco Sverige, Tekniska verken i Linköping, Uniper, Vattenfall R&D, Vattenfall Vattenkraft, Voith Hydro, WSP Sverige, Zink-gruvan, and Å F Industry.

References

Alobaidi, I. and Hoare, D. (1994), "Factors affecting the pumping of fines at the subgrade subbase interface of highway pavements: A laboratory study", *Geosynthetics Int.*, **1**(2), 221-259. https://doi.org/10.1680/gein.1.0010.

Alobaidi, I. and Hoare, D.J. (1996). "The development of pore water pressure at the subgrade-subbase interface of a highway pavement and its effect on pumping of fines", *Geotext. Geomembranes*, **14**(2), 111-135. https://doi.org/10.1016/0266-1144(96)84940-5.

Baki, M.A.L., Rahman, M.M., Lo, S.R. and Gnanendran, C.T. (2012), "Linkage between static and cyclic liquefaction of loose sand with a range of fines contents", *Can. Geotech. J.*, **49**(8), 891-906. https://doi.org/10.1139/t2012-045.

Bedin, J., Schnaid, S., Fonseca, A.V.D. and Filho, L.D.M.C. (2012), "Gold tailings liquefaction under critical state soil mechanics", *Géotechnique*, **62**(3), 263-267. https://doi.org/10.1680/geot.10.P.037.

Bella, G. (2021), "Water retention behaviour of tailings in unsaturated conditions." *Geomech. Eng.*, **26**(2), 117-132. https://doi.org/10.12989/gae.2021.26.2.117.

Cai, Y., Gu, C., Wang, J., Juang, C.H., Xu, C. and Hu, X. (2013), "One-Way cyclic triaxial behavior of saturated clay: comparison between constant and variable confining pressure", *J. Geotech. Geoenviron. Eng.*, **139**(5), 797-809. https://doi.org/10.1061/(ASCE)GT.1943-5606.0000760.

Christopher, B.R., Schwartz, C.W., Boudreaux, R. and Berg, R.R. (2006), "*Geotechnical aspects of pavements*", United States. Federal Highway Administration.

Dash, H. and Sitharam, T. (2011), "Cyclic liquefaction and pore pressure response of sand-silt mixtures." *Geomech. Eng.*, **3**(2), 83-108. https://doi.org/10.12989/gae.2011.3.2.083.

Do, T.M. (2021), "Excess pore water pressure generation in fine granular materials and migration of particles under cyclic loading - a laboratory study", Licenciate Thesis, Luleå University of Technology, Luleå.

Duong, T.V., Tang, A.M., Cui, Y.J., Trinh, V.N., Dupla, J.C., Calon, N., Canou, J. and Robinet, A. (2013), "Effects of fines and water contents on the mechanical behavior of interlayer soil in ancient railway sub-structure", *Soils Found.*, **53**(6), 868-878. https://doi.org/10.1016/j.sandf.2013.10.006.

Festugato, L., Fourie, A. and Consoli, N.C. (2013), "Cyclic shear response of fibre-reinforced cemented paste backfill", *Géotechnique Lett.*, **3**(1), 5-12. https://doi.org/10.1680/geolett.12.00042.

Förstner, U. (1999), "Introduction." *Environmental Impacts of Mining Activities: Emphasis on Mitigation and Remedial Measures*, J. M. Azcue, ed., Springer Berlin Heidelberg, Berlin, Heidelberg.

Geremew, A.M. and Yanful, E.K. (2012), "Laboratory investigation of the resistance of tailings and natural sediments to cyclic loading", *Geotech. Geol. Eng.*, **30**(2), 431-447. https://doi.org/10.1007/s10706-011-9478-x.

Geremew, A.M. and Yanful, E.K. (2013), "Dynamic properties and influence of clay mineralogy types on the cyclic strength of mine tailings", *Int. J. Geomech.*, **13**(4), 441-453. https://doi.org/10.1061/(ASCE)GM.1943-5622.0000227.

Gu, C., Wang, J., Cai, Y., Sun, L., Wang, P. and Dong, Q. (2016), "Deformation characteristics of overconsolidated clay sheared under constant and variable confining pressure", *Soils Found.*, **56**(3), 427-439. https://doi.org/10.1016/j.sandf.2016.04.009.

Hu, L., Wu, H., Zhang, L., Zhang, P. and Wen, Q. (2017). "Geotechnical properties of mine tailings", *J. Mater. Civil Eng.*, **29**(2), 04016220. https://doi.org/10.1061/(ASCE)MT.1943-5533.0001736.

Hyde, A.F., Higuchi, T. and Yasuhara, K. (2006), "Liquefaction, cyclic mobility, and failure of silt", *J. Geotech. Geoenviron. Eng.*, **132**(6), 716-735. https://doi.org/10.1061/(ASCE)1090-0241(2006)132:6(716).

Indraratna, B., Singh, M., Nguyen, T.T., Leroueil, S., Abeywickrama, A., Kelly, R. and Neville, T. (2020), "Laboratory study on subgrade fluidization under undrained cyclic triaxial loading", *Can. Geotech. J.*, **57**(11), 1767-1779. https://doi.org/10.1139/cgj-2019-0350.

Ishihara, K., Troncoso, J., Kawase, Y. and Takahashi, Y. (1980), "Cyclic strength characteristics of tailings materials", *Soils Found.*, **20**(4), 127-142. https://doi.org/10.3208/sandf1972.20.4_127.

James, M., Aubertin, M., Wijewickreme, D. and Ward, W. (2011), "A laboratory investigation of the dynamic properties of tailings", *Can. Geotech. J.*, **48**(11), 1587-1600. https://doi.org/10.1139/t11-060.

Kammerer, A.M., Pestana, J.M. and Seed, R.B. (2002), "Geotechnical Engineering Report No UCB/GT/02-01", Department of Civil and Environmental Engineering University of California, Berkeley.

Kermani, B., Xiao, M., Stoffels, S.M. and Qiu, T. (2019), "Measuring the migration of subgrade fine particles into subbase using scaled accelerated flexible pavement testing – a laboratory study", *Road Mater. Pavement Design*, **20**(1), 36-57. https://doi.org/10.1080/14680629.2017.1374995.

Kheirbek-Saoud, S. and Fleureau, J.M. (2012), "Liquefaction and post-liquefaction behaviour of a soft natural clayey soil", *Geomech. Eng.*, **4**(2), 121-134. https://doi.org/10.12989/gae.2012.4.2.121.

Knutsson, R. and Laue, J. (2016), "Numerical analysis of Aitik pier S1 subjected to dynamic loads", Lulea University of Technology, Technical Report.

Kwan, W.S. and Mohtar, C.E. (2018), "A review on sand sample reconstitution methods and procedures for undrained simple shear test", *Int. J. Geotech. Eng.*, **14**(8), 1-9. https://doi.org/10.1080/19386362.2018.1461988.

Ladd, R. (1978), "Preparing test specimens using undercompaction", *Geotech. Test J.*, **1**(1), 16-23. https://doi.org/10.1520/GTJ10364J.

Lade, P.V. (2016). "Preparation of Triaxial Specimens", *Triaxial Testing of Soils*, 211-237.

Li, Y., Yang, Y., Yu, H.S. and Roberts, G. (2017), "Correlations between the stress paths of a monotonic test and a cyclic test under the same initial conditions", *Soil Dyn. Earthq. Eng.*, **101**, 153-156. https://doi.org/10.1016/j.soildyn.2017.07.023.

Moriwaki, Y., Akky, M.R., Ebeling, A.M, Idriss, I.M. and Ladd, R.S. (1982), *Cyclic strength and properties of tailings slimes*, American Society of Civil Engineers (ASCE), New York

Moses, G.G., Rao, S.N. and Rao, P.N. (2003), "Undrained strength behaviour of a cemented marine clay under monotonic and

cyclic loading", *Ocean Eng.*, **30**(14), 1765-1789. https://doi.org/10.1016/S0029-8018(03)00018-0.

Peters, G. and Verdugo, R. (2003), "Seismic design considerations of tailings dams", *Soil rock America 2003: Proceedings of the 12th panamerican conference on soil mechanics and geotechnical engineering*.

Sarsby, R.W. (2013), "Tailings dams", *Environmental Geotechnics*, 2nd Ed., 365-391.

Selig, E.T. and Chang, C.S. (1981), "Soil failure modes in undrained cyclic loading", *J. Geotech. Geoenviron. Eng.*, **107**(5). https://doi.org/10.1061/AJGEB6.0001128.

Shajarati, A., Sørensen, K.W. and Ibsen, L.B. (2012), "Manual for cyclic triaxial test", Department of Civil Engineering, Aalborg University. DCE Technical reports No. 114.

Sonmezer, Y.B. (2019), "Investigation of the liquefaction potential of fiber-reinforced sand", *Geomech. Eng.*, **18**(5), 503-513. https://doi.org/10.12989/gae.2019.18.5.503.

Sonmezer, Y.B., Akyuz, A. and Kayabali, K. (2020), "Investigation of the effect of grain size on liquefaction potential of sands", *Geomech. Eng.*, **20**(3), 243-254. https://doi.org/10.12989/gae.2020.20.3.243.

Suazo, G., Fourie, A., Doherty, J. and Hasan, A. (2016). "Effects of confining stress, density and initial static shear stress on the cyclic shear response of fine-grained unclassified tailings", *Géotechnique*, **66**(5), 401-412. https://doi.org/10.1680/jgeot.15.P.032.

Tsuchida, H. (1970), "Prediction and countermeasure against the liquefaction in sand deposits", *Proc., Abstract of the seminar in the Port and Harbor Research Institute*, 31-333.

Verdugo, R. (2009), "Seismic performance based-design of large earth and tailing dams", *International Conference on Performance-Based Design in Earthquake*, 41-60.

Vernay, M., Morvan, M. and Breul, P. (2016), "Influence of saturation degree and role of suction in unsaturated soils behaviour: application to liquefaction", *E3S Web Conf.*, 9, 14002.

Vick, S.G. (1983), *Planning, design and analysis of tailings dams*, Wiley series on geotechnical engineering. Wiley, New York.

Wang, B., Zen, K., Chen, G. and Kasama, K. (2012), "Effects of excess pore pressure dissipation on liquefaction-induced ground deformation in 1-g shaking table test", *Geomech. Eng.*, **4**(2), 91-103. https://doi.org/10.12989/gae.2012.4.2.091.

Wang, Y., Gao, Y., Li, B., Fang, H., Wang, F., Guo, L. and Zhang, F. (2017), "One-way cyclic deformation behavior of natural soft clay under continuous principal stress rotation", *Soils Found.*, **57**(6), 1002-1013. https://doi.org/10.1016/j.sandf.2017.08.027.

Wheeler, L.N., Take, W.A. and Hoult, N.A. (2017), "Performance assessment of peat rail subgrade before and after mass stabilization", *Can. Geotech. J.*, **54**(5), 674-689. https://doi.org/10.1139/cgj-2016-0256.

Wijewickreme, D., Sanin, M.V. and Greenaway, G.R. (2005), "Cyclic shear response of fine-grained mine tailings", *Can. Geotech. J.*, **42**(5), 1408-1421. https://doi.org/10.1139/t05-058.

Zardari, M.A., Mattsson, H., Knutsson, S., Khalid, M.S., Ask, M., and Lund, B. (2017), "Numerical analyses of earthquake induced liquefaction and deformation behaviour of an upstream tailings dam", *Adv. Mater. Sci. Eng.*, **2017**, 1-12. https://doi.org/10.1155/2017/5389308.

Zhang, C., Yang, C.H. and Bai, S.W. (2006), "Experimental study on dynamic characteristics of tailings material", *Rock Soil Mechanics-Wuhan*, **27**, 35-40.

List of notations

CSR	Cyclic stress ratios
PWP	Pore water pressure
f	Frequency
r_u	Excess pore water pressure ratio
σ_c'	Effective confining pressure
D_{50}	Corresponding particle size when the cumulative percentage reaches 50%
θ	Empirical constant determined from laboratory testing in Eq. (2)
N	Number of cycles
N_{Acc}	Number of cycles at which the incremental increase of excess PWP ratio per cycle starts accelerating
a, b	Model parameters in Eq. (3)
D_r	Relative density
q_{cyc}	Amplitude of cyclic stress
p'	Effective stress
q	Deviatoric stress
ε_a	Cyclic axial strain